Response Characteristics of Base-isolated Structure with Hardening-stopper Type Fail-safe Devices

Mitsuru OHHIRA, Shigeo HIGAKI
Power Reactor & Nuclear Fuel Development Corporation, Tokyo, Japan
Masuhiko KOBATAKE, Yasuo NITTA
Shimizu Corporation, Tokyo, Japan

1. INTRODUCTION

In this study, a fail-safe mechanism for backing up the reliability of an isolator device is being developed predicated on the application of a base isolation system to nuclear fuel facilities. "Fail-safe" is often understood to mean that when a device loses its function, a separate mechanism will work in order that there will be no trouble with regard to safety. However, since it may be considered extremely difficult to support loads without any trouble when the base isolation device itself loses its function, the term will be used here to mean that the base isolation device is supported so that it will not lose its function. The two points below will be made the objectives of design as workings of the fail-safe system in this study.

1) Response Displacement Control : Suppresses excessive deformation of the base isolation device even in case of input of an earthquake greater than the design seismic force to prevent destruction of the base isolation device, superstructure, and connected piping.
2) Response Acceleration Control : Reduces acceleration transmitted to the superstructure insofar as possible by action of the fail-safe mechanism.

Characteristics tests and analyses, and earthquake observations using reduced-scale model have now been carried out to grasp the response characteristics of a base isolation system combining high-damping rubber bearings and hardening-stopper type fail-safe mechanisms, and the results will be reported below.

2. CHARACTERISTICS TESTS OF DEVICE

In order to obtain a grasp of the basic characteristics of a base isolation system combining high-damping rubber bearings and hardening-stopper type fail-safe mechanisms, basic characteristics tests were performed using reduced scale specimens.

2.1 SPECIMENS AND TESTING METHOD

As specimens, reduced high-damping rubber bearing (rated load : 20 tf) of 1/5-scale of high-damping rubber bearings (rated load : 500 tf) used in actual buildings and hardening-stopper type fail-safe devices to be combined with the bearings were trial-manufactured. A reduced high-damping rubber bearing is shown in Fig. 1. For connections, the two kinds of methods of fixed-flange type and dowel-pinned type were adopted.

The fail-safe device is set in ring shape around the rubber bearing as shown in Fig. 2. When the relative displacement of the rubber bearing reaches a given level of deformation (δ=8cm, γ=200%), it will come in contact with the stopper part. The stopper part was tested using several varieties of elastic rubber. The three representative types are shown in Fig. 3.

The loading method consisted of incremental and alternating cyclic loading by displacement control of a horizontal actuator while applying the specified bearing pressure to the rubber bearing by vertical actuator.

2.2 TEST RESULTS

The restoring force characteristics of the fail-safe device are shown in Fig. 4. The device begins to act at horizontal displacement of 8 cm. The initial stiffness of the device is small, but from around 11 cm the stiffness is increasing smoothly.

The hysteresis loops up to large deformation of the high-damping rubber bearings are shown in Fig. 5. The rubber bearing of fixed-flange type reached the ultimate state with cracks occurring in the rubber at horizontal displacement of 16.8 cm (γ = 420%). The dowel-pinned type showed the phenomenon of separation of the dowel-connected plane from around 8.0 cm (γ = 200%), and at 16.0 cm (γ = 400%) the dowel-connected plane became completely separated. However, failure of rubber did not occur.

Fig. 6 shows skeleton curves of the two types. Up to shear strain of 200% when the dowel-connected plane of the dowel-pinned type begins to separate, the two types indicate practically the same characteristics, but in the strain range above that the fixed-flange type has a greater tendency for hardening than the dowel-pinned type. The specimens used in these ultimate tests had already been subjected to deformation hystereses up to horizontal displacement 12.0 cm, so that, for the sake of reference, curves at initial loading were also shown. It can be seen that stiffness is reduced approximately 30% compared with initial loading with a high-damping rubber bearing after a large deformation has been sustained. The skeleton curves in case of addition of fail-safe devices are also shown in these figures.

3. RESPONSE ANALYSES

Modeling of the restoring force characteristics of base isolation devices was done based on the results of the characteristics tests and response analyses by one-mass system models as shown in Fig. 7 were performed to obtain the response characteristics of the base isolation system with a hardening-stopper. In this case, models were made converting to the constant for an actual-size rubber bearing for rated load of 500 tf, based on the reduction ratio of specimens used in characteristics tests. Input seismic waves were El Centro 1940 NS and Hachinohe 1968 EW.

The restoring force characteristics of high-damping rubber bearings were modeled as strain-dependent-type modified bi-linear models composed of skeleton curves and hysteresis loops, which are defined by the characteristic values of shear stress τ_0, equivalent damping factor h_{eq} and Y-axis intercept stress τ_D shown in Fig. 8. These characteristic values are expressed as functions by shear strain γ. The shear stress-strain relationship is shown in Fig. 9, the equivalent damping ratio-strain relationship in Fig. 10, and the Y-axis intercept stress-strain relationship in Fig. 11. The shear stress in the large deformation range (γ>200%) of the high-damping rubber bearing has a tendency to be decreased by approximately 30% of the initial shear stress due to repetitions of deformation. Because of this, these characteristic values were evaluated for the loops of the third cycles of the characteristics tests. And for the effect of the initial loadings, the commensurate hysteresis loops were

added after that. The restoring force characteristics of high-damping rubber bearings defined according to the above are shown in Fig. 12.

For the restoring force characteristics of the fail-safe device, the hardening curves in Fig. 13 were assumed, referring to the results of characteristics tests. And varying yield points, two kinds of hysteresis loops shown in Fig. 14 were used.

The maximum response values by analyses are plotted on the skeleton curves of all models in Fig. 15. There are differences in responses depending on the seismic wave, but as an overall trend, when the fail-safe device acts, the maximum response displacement is suppressed but the maximum response shear force is increased up to 1.1 - 3.0 times, compared with the response of the model without fail-safe device

4. EARTHQUAKE OBSERVATION BY REDUCED-SCALE MODEL

Outdoor earthquake observations were carried out with a reduced-scale base-isolated model to grasp the earthquake response characteristics of base-isolated structures having hardening-stopper type fail-safe mechanisms. The superstructure of the base-isolated model is shown in Fig. 16. Four each of the high-damping rubber bearings and hardening-stopper type fail-safe devices shown in Fig. 17 have been set in this structure. Prior to earthquake observations, the basic characteristics of the model were grasped performing shaking table tests. After that it was installed on a reinforced concrete mat constructed in Tokai site of Power Reactor and Nuclear Fuel Development Corporation. Totally 50 earthquakes have been observed so far and the response characteristics of the base-isolated structure and surrounding ground have been ascertained. However, an earthquake in which the relative displacement reached the activating displacement for the fail-safe mechanism (25 mm) has not been observed as yet.

The response waves of the base-isolated structure model observed in the earthquake on May 3, 1990 (M5.8, Δ7km) are shown in Fig. 18. During this earthquake, the relative displacement became 8.8 mm. The results of simulation analyses performed using the characteristics values obtained in shaking table tests simulates the observed waves well.

5. CONCLUSION

1) The characteristics of high-damping rubber bearings during large deformations was successfully grasped through tests, and it could be modeled by a newly designed restoring force characteristics model.
2) It has been succeeded in accumulating design data concerning displacement responses and shear forces of base isolation devices when stoppers act, by performing response analyses of base-isolated structures with fail-safe devices using the results of characteristics tests.
3) Efforts will be made for development of a fail-safe mechanism to back up the reliability of base isolation devices, through grasping of the characteristics of the devices and continuing further with earthquake observations using reduced-scale base-isolated models with hardening-stopper type fail-safe mechanisms.

REFERENCE

Ohhira,M., Higaki,S., Teramura,A., Nakamura,T., Kobatake,M. and Hisano,M.(1990) Earthquake Response Characteristics of Base-isolated Building Models with File-safe Davices. The Eighth Japan Earthquake Engineering Symposium, Tokyo.

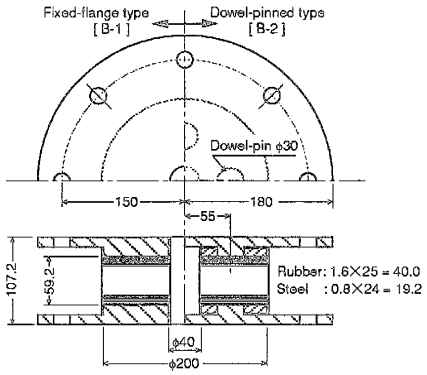

Fig.1 Reduced High-damping Rubber Bearing

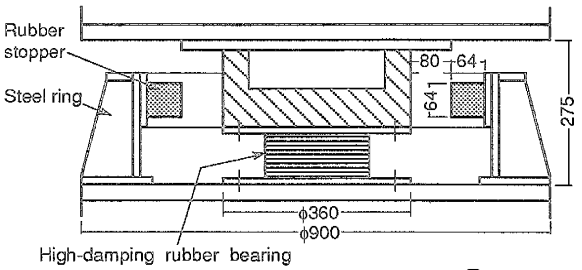

Fig.2 Hardening-stopper Type Fail-safe Device

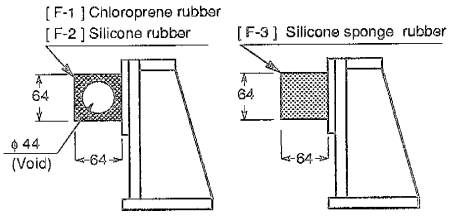

Fig.3 Rubber Stopper Part

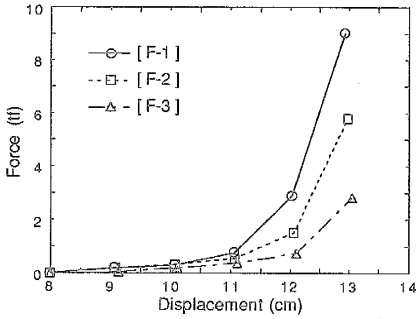

Fig.4 Characteristics of Fail-safe

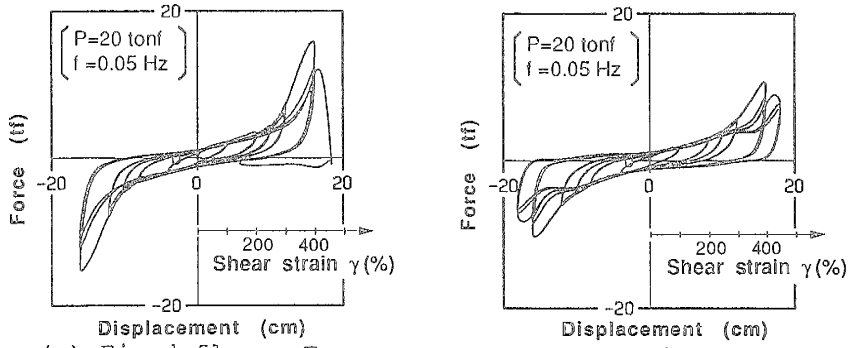

Fig.5 Hysteresis Loops of High-damping Rubber Bearing

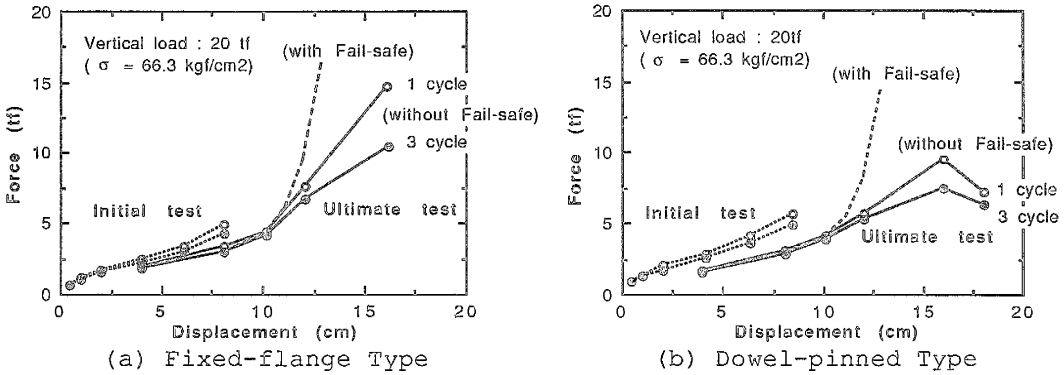

Fig.6 Skeleton Curves of High-damping Rubber Bearing

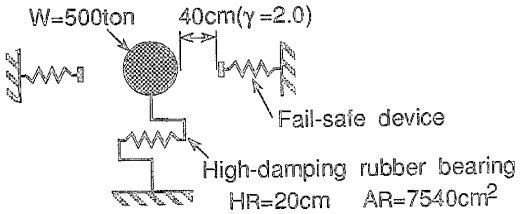

Fig.7 Response Analysis Model

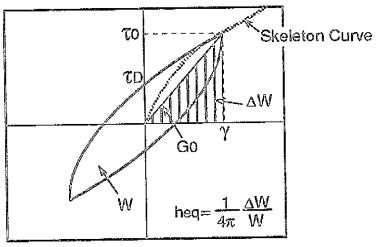

Fig.8 Characteristics Values

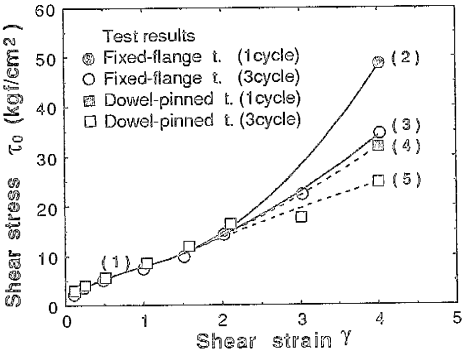

[0.1≦ γ ≦1.5]

(1) $\tau_0 = 1.47 + 10.6\gamma - 6.45\gamma^2 + 2.26\gamma^3$

[1.5< γ ≦4.0]

Fixed-flange type

(2) $\tau_0 = 8.30 - 3.58\gamma + 3.38\gamma^2$ (Initial loading curve)

(3) $\tau_0 = 3.27 + 3.13\gamma + 1.14\gamma^2$ (Cyclic loading curve)

Dowel-pinned type

(4) $\tau_0 = 2.44 + 4.24\gamma + 0.774\gamma^2$ (Initial loading curve)

(5) $\tau_0 = -0.126 + 7.66\gamma - 0.366\gamma^2$ (Cyclic loading curve)

Fig.9 Shear Stress-Strain Relationship

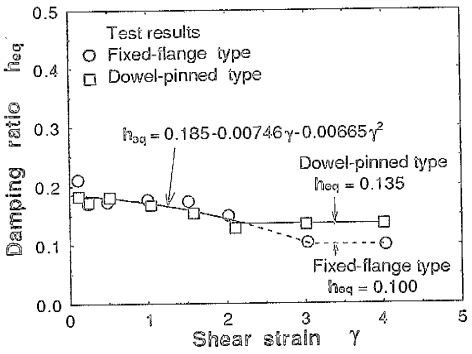

Fig.10 Equivalent Damping Ratio

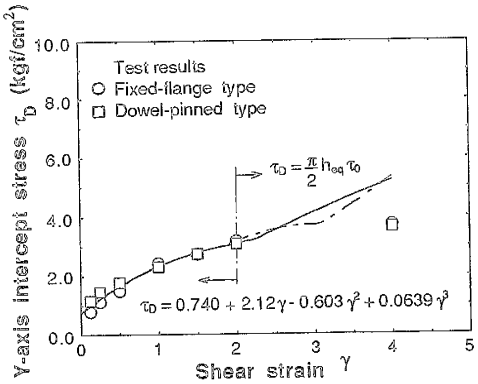

Fig.11 Y-axis Intercept Stress

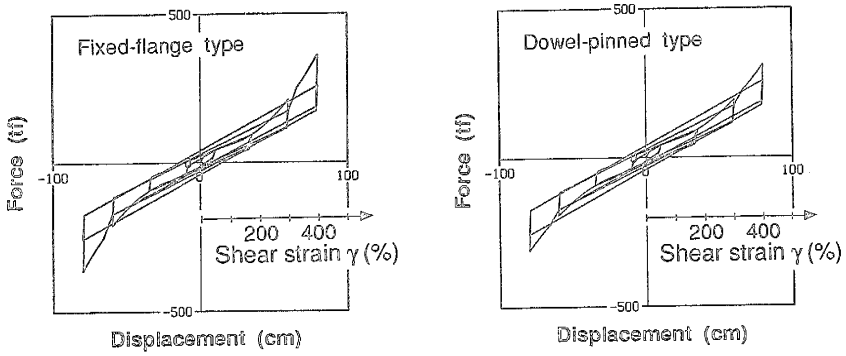

Fig.12 Restoring Force Characteristics of High-damping Rubber Bearing

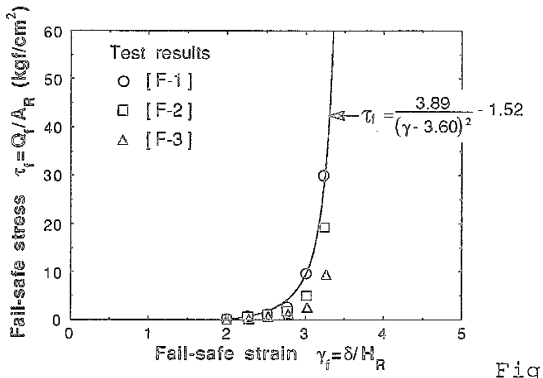

Fig.13 Fail-safe Stress-Strain Relationship

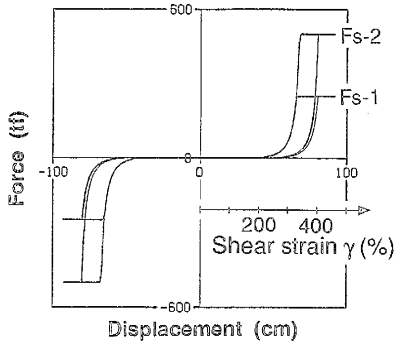

Fig.14 Restoring Force Characteristics of Fail-safe Device

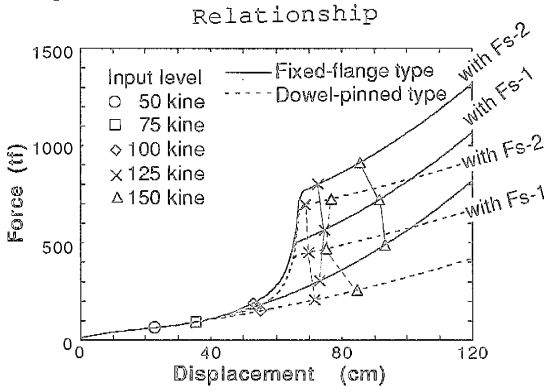

(a) El Centro 1940 NS Input

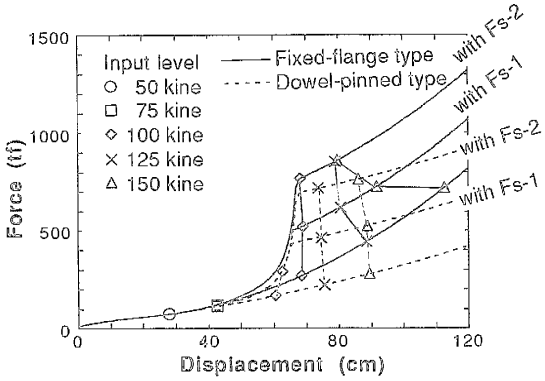

(b) Hachinohe 1968 EW Input

Fig.15 Maximum Response Values by Analyses

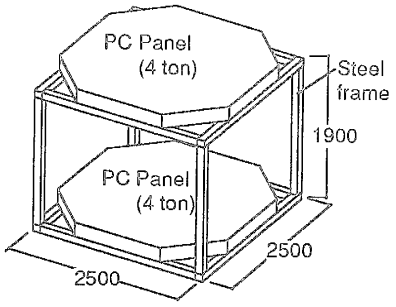

Fig.16 Model for Earthquake Observation

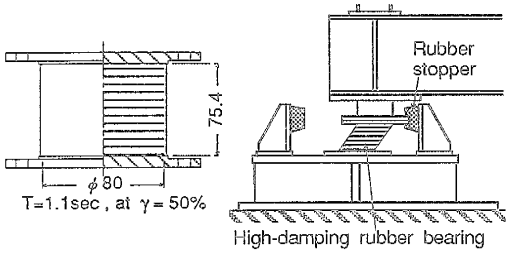

Fig.17 Base Isolation Device

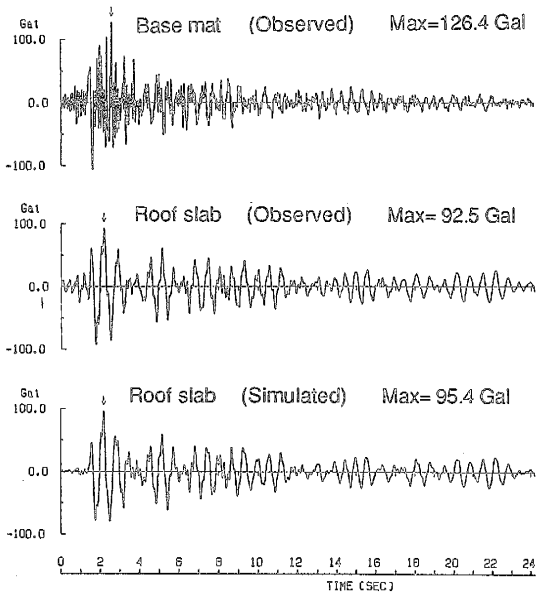

Fig.18 Time History Records of the Earthquake on May 3,1990